IFSCC 2025 full paper (ABSTRACT N° IFSCC2025-1767)

"Implementation and Validation of a Pigmentation Model Using B16-F10 Melanoma Cells for Dermatological Applications"

Hanan Osman-Ponchet [1,*], Fadéla Benzaoui [1], Manon Barthe [1], Jean-Paul Thénot [1], and Sandrine Troussieux [2,]

[1] Laboratoires PKDERM, Grasse, France; [2]Amoéba, Chassieu, France

1. Introduction

Skin hyperpigmentation disorders—including melasma, post-inflammatory hyperpigmentation (PIH), and solar lentigines—are pervasive dermatological concerns driven by dysregulated melanogenesis triggered by UV exposure, hormonal fluctuations, or inflammation. These conditions significantly impact patients' quality of life, fueling a global depigmenting cosmetics market projected to reach USD 2.02 billion by 2030 (1).

Central to these disorders is melanogenesis: the biochemical process where epidermal melanocytes synthesize melanin through tyrosinase (TYR)-governed enzymatic cascades. While melanin provides critical photoprotection against UV-induced DNA damage, its overproduction or uneven distribution leads to cosmetically problematic hyperpigmentation (2). Current tyrosinase inhibitors (e.g., kojic acid, hydroquinone) face limitations in stability, safety, and regulation (3), underscoring the need for innovative *in vitro* models to accelerate cosmetic discovery.

While primary melanocytes and melanoma cell lines have been used to study melanogenesis, they suffer from poor reproducibility, scalability, and genetic tractability. The murine B16-F10 melanoma cell line addresses these limitations through:

- Exceptional melanogenic capacity (>5× higher than primary melanocytes),
- Rapid proliferation in standard culture,
- High responsiveness to stimuli like 3-isobutyl-1-methylxanthine (IBMX) (4,5).

IBMX, a phosphodiesterase inhibitor, potently upregulates melanogenesis via the **cAMP/protein kinase A (PKA)/ cAMP-responsive element-binding protein (CREB)/ microphthalmia-associated transcription factor (MITF) pathway**:

1. IBMX inhibits PDE-mediated cAMP degradation resulting in increased intracellular cAMP
2. cAMP activates PKA which phosphorylates the CREB

3. Phospho-CREB binds the MITF promoter, leading to increased MITF expression
4. MITF transcriptionally activates melanogenic enzymes (TYR, TRP-1, TRP-2), resulting in increased melanin synthesis (6,7).

Despite IBMX's established role, existing B16-F10 models suffer critical limitations:

- **Reproducibility challenges**: Unstandardized culture conditions (e.g., variable tyrosine levels in media) cause false positives/negatives (2)
- **Incomplete mechanistic validation**: Most studies use only chemical inhibitors (e.g., kojic acid), lacking genetic confirmation (8)
- **Low throughput**: Poor adaptability for screening complex botanical extracts/lysates.

In this study, we bridge these gaps with a multi-validated B16-F10/IBMX platform featuring:

- **Tyrosine-optimized media** to standardize melanogenesis,
- **Dual chemical/genetic validation** (kojic acid + *TYR* siRNA),
- **High-throughput screening** of novel sustainable actives (*Willaertia magna* C2c Maky lysate).

This model uniquely integrates academic rigor with industrial scalability, enabling reliable discovery of next-generation depigmenting agents.

2. Materials and Methods

2.1. Cell Culture, Media Optimization, and Maintenance

The B16-F10 melanoma cell line (ATCC® CRL-6475™) was cultured under tyrosine-controlled conditions essential for melanogenesis studies. Tyrosine serves as the primary substrate for melanin synthesis via tyrosinase catalysis. Uncontrolled variation in basal tyrosine concentrations (DMEM ≈104 µM vs. DMEM/F12 ≈55 µM) significantly impacts melanogenesis endpoints, necessitating media-specific standardization (2). Media formulations were rigorously selected based on tyrosine content:

- Model Validation: **High-glucose DMEM** (4.5 g/L glucose; Gibco #31966-021 or VWR #392-0416) containing 104 µM tyrosine
- Application Studies: **DMEM/F12** (1:1 mixture; VWR #31331-028) containing 55 µM tyrosine.

All media were supplemented with 10% fetal bovine serum (FBS) (Gibco™) and 1× antibiotic-antimycotic (10,000 U/mL penicillin, 10,000 µg/mL streptomycin, 25 µg/mL amphotericin B; Gibco™ #15240062).

Cells were grown in 75 cm² flasks (Corning®) at 37°C under 5% CO_2 (ThermoScientific MIDI 40). Subculturing occurred every 3–4 days at 80% confluence.

Cell morphology and melanosome formation were monitored using a Nikon Eclipse Ti-e inverted microscope equipped with NIS-Elements AR software (v5.11.03). Imaging was performed to assess viability and confluence, and to document melanosome accumulation in B16-F10 cells post-treatment.

2.2. B16-F10 Cell Treatment Protocols

B16-F10 cells (passages P6–P16) were seeded in 24-well plates at a density of 50,000 cells/well using tyrosine-controlled media (Section 2.1). Following 24 h incubation to ensure adherence, treatments were initiated with specific concentration ranges and temporal parameters across three experimental series:

1. ***IBMX Optimization***

- Concentrations: 10, 100, 1000 µM IBMX
- Controls: Vehicle (0.1% DMSO)
- Duration: 24 h and 48 h
- Replicates: 7 independent experiments (n = 3 wells/condition)

2. Kojic Acid Validation

- Kojic acid (100 and 200 µM)
- Duration: 48 h
- Replicates: 10 independent experiment

B16-F10 were treated with kojic acid alone or with kojic acid ± 100 µM IBMX. Cells treated with the vehicle served as control.

3. Cosmetic Ingredient Screening

A novel bioactive ingredient was developed for cosmetic and dermocosmetic applications, leveraging the patented use of a lysate derived from *Willaertia magna* C2c Maky. This natural, biosourced material is classified as a hydrobiome-derived postbiotic, originating from thermal spring waters in the French Alps (9).

Evaluation of Melanogenesis Modulation:

The effect of the *Willaertia magna* C2c Maky lysate on melanogenesis was assessed using B16-F10 murine melanoma cells under the following conditions:

- Test substance: *Willaertia magna* C2c Maky lysate
- Concentrations: 0.001% (w/v)
- Duration: 48 h
- Replicates: Three independent biological replicates

B16-F10 were exposed to *Willaertia magna* lysate alone, *Willaertia magna* lysate + 100 µM IBMX, or 100 µM Kojic acid ± 100 µM IBMX. Cells exposed to the vehicle served as control. All incubations were conducted at 37°C and 5% CO_2 in high-glucose DMEM containing 104 µM tyrosine.

2.3. Genetic Validation via TYR siRNA Knockdown

To confirm model specificity for tyrosinase-dependent melanogenesis, targeted gene silencing was performed using siRNA against the *Tyr* gene (tyrosinase). B16-F10 cells were seeded in 12-well plates at a density of 100,000 cells/well in high-glucose DMEM (Gibco™) and incubated for 24 h to ensure adherence. Transfection complexes were prepared by combining On-TARGETplus SMARTpool siRNA (containing four distinct sequences targeting murine *Tyr*; Horizon Discovery) with DharmaFECT 1 Transfection Reagent (Horizon Discovery) in serum-free medium, achieving final concentrations of 100 nM siRNA and 0.2% (v/v) transfection reagent. After 20 min incubation at room temperature, complexes were added to cells, with scrambled siRNA serving as the negative control.

The transfection period lasted 6 h at 37°C under 5% CO_2, after which the medium was replaced with fresh complete DMEM containing 100 µM IBMX to initiate melanogenesis. Four experimental conditions were evaluated in duplicate wells: (1) untreated control (baseline), (2) IBMX alone (100 µM), (3) IBMX (100 µM) plus kojic acid (200 µM), and (4) Tyr siRNA-transfected cells with IBMX (100 µM). The treatment duration was 48 hours following the addition of IBMX. Following treatment, cells were harvested and centrifuged at 500 × g for 5 min. Resulting pellets were divided equally for parallel analyses: one half underwent RNA isolation using the SV Total RNA Isolation System (Promega #Z3105) for molecular characterization, while the other half was reserved for melanin and protein quantification.

For transcriptional validation, 500 ng of total RNA was reverse-transcribed using the High Capacity cDNA RT Kit (ThermoFisher #4368813). Quantitative real-time PCR was performed in

triplicate reactions using TaqMan Universal Master Mix II (Applied Biosystems #4326708) with *Tyr*-specific probes (Mm00495817_m1) and *GAPDH* endogenous control (Mm99999915_g1). Relative *Tyr* expression was calculated via the ΔΔCt method normalized to glyceraldehyde-3-phosphate dehydrogenase (*GAPDH)* gene.

2.4. Melanin Quantification and Tyrosinase Activity Assays

- ***Melanin Quantification***

Post-treatment, B16-F10 cells in 24-well plates underwent two washes with 500 µL Dulbecco's Phosphate-Buffered Saline (DPBS) without calcium and magnesium. Melanin extraction employed two validated protocols: the detached cell method, where cells were scraped in 500 µL DPBS and centrifuged (14,000 rpm, 5 min, 4°C), followed by pellet lysis in 120 µL 1N NaOH; and the direct lysis method, involving addition of 250 µL 1N NaOH directly to wells. Both methods proceeded with incubation at 80°C for 1 h under 350 rpm agitation (Labnet AccuTherm). Following centrifugation (14,000 rpm, 10 min, 4°C), supernatants were transferred to 96-well plates: 50 µL for the detached method or 100 µL for direct lysis. Absorbance was measured at 405 nm, 450 nm, and 490 nm using a GloMax Explorer spectrophotometer (Promega France), with 405 nm serving as the primary melanin quantification wavelength. Melanin content was calculated against a synthetic melanin standard curve (0–200 µg/mL) and normalized to total cellular protein, with all samples analyzed in duplicate (n=2).

- ***Tyrosinase Activity Assay***

Cells were washed twice with DPBS and lysed in 100 µL ice-cold 1% Triton X-100 (45 min, 4°C) to preserve enzyme activity. Subsequently, 20 µL of lysate was reacted with 100 µL of 2 mM L-DOPA in PBS (pH 6.8) in 96-well plates. Dopachrome formation was kinetically monitored at 490 nm with measurements every 5 min for 55 min at 37°C using the GloMax Explorer. Tyrosinase activity was quantified as the area under the kinetic curve (AUC), calculated from the time-dependent absorbance profile (OD_{490} × min) using the trapezoidal method. All samples were analyzed in duplicate (n=2).

2.5. Statistical Analysis

All data are presented as mean ± standard deviation (SD). Statistical analyses were performed using Excel Analysis ToolPack. For comparisons between two groups, the Mann-Whitney U test (non-parametric) was applied. For comparisons among three or more groups, one-way analysis of variance (ANOVA single factor) was employed followed by Tukey's post-hoc test for multiple comparisons. A significance threshold of $p < 0.05$ was applied for all analyses, with exact p-values reported where applicable ($p < 0.05$, $p < 0.01$, $p < 0.001$).

3. Results

3.1. Establishment and Optimization of the B16-F10 Pigmentation Model

3.1.1. IBMX-Induced Melanogenesis

The IBMX-stimulated B16-F10 model exhibited robust, dose- and time-dependent melanogenesis. Initial wavelength scanning (405, 450, 490 nm) confirmed optimal melanin detection at 405 nm (longer wavelength), which was subsequently adopted for all measurements. As shown in Fig. 1a, melanin induction after 24h IBMX exposure remained modest across concentrations. In contrast, 48h stimulation (Fig. 1b) demonstrated a pronounced dose-dependent response, with melanin content peaking at 100 µM IBMX (2.3-fold increase vs. control, $p<0.05$, n=6) and plateauing at 1000 µM. Time-course analysis confirmed maximal accumulation at 48h. Consequently, 100 µM IBMX with 48h stimulation and 405 nm quantification were standardized for all subsequent experiments.

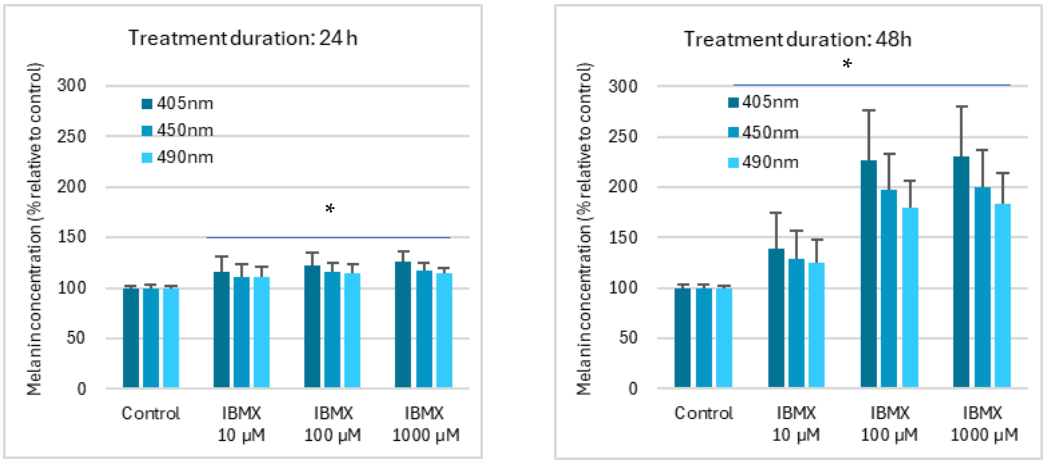

(**a**) (**b**)

Figure 1. Dose- and time-dependent melanogenesis in IBMX-stimulated B16-F10 cells. (a) Melanin content after 24h IBMX exposure; (b) Melanin content after 48h IBMX exposure (optimal induction. Data represent the mean and standard deviation (n=14, seven independent experiments in duplicate). * $p<0.05$.

Concomitant with melanogenesis, IBMX triggered time- and dose-dependent tyrosinase activation (Figure 2). At 24h, IBMX induced only modest tyrosinase upregulation (14–19% increase across concentrations), consistent with limited melanin synthesis (Figure 2a). In stark contrast, 48h exposure elicited robust enzyme activation (39–108% increase), with mean maximal activity 46% higher than at 24h (Figure 2b). Dose-response analysis confirmed tyrosinase activity plateaued at 1000 µM IBMX, where it reached 1.8-fold higher levels versus untreated controls.

This synchronized peak at 48h aligned temporally with melanin plateau, confirming coordinated pathway activation. Consequently, 100 µM IBMX/48h was established as the standardized induction window for all downstream assays.

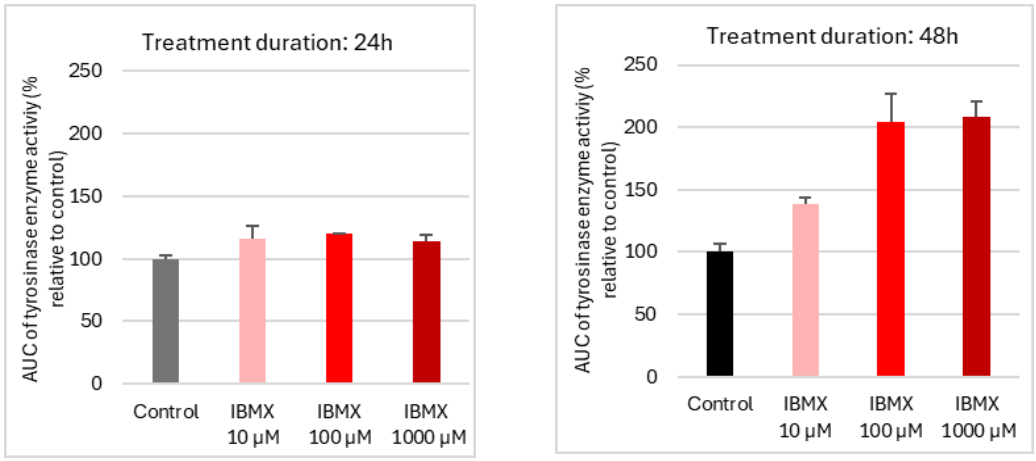

(**a**) (**b**)

Figure 2. Time- and dose-dependent effects of IBMX on tyrosinase activation in B16-F10 cells. (a) Tyrosinase activity after 24h IBMX exposure shows limited induction. (b) Robust 48h response demonstrates dose-dependent amplification, with activity plateauing at 1000 µM IBMX. Data represent mean and SD; n=4 (two independent experiments in duplicate).

3.1.2. Critical Role of Tyrosine Standardization in Melanogenic Output

Media tyrosine concentration governed IBMX-driven melanogenesis through synergistic substrate-enzyme modulation. Under standardized induction (100 µM IBMX, 48h), high-tyrosine DMEM (104 µM) generated 23.8% greater absolute melanin accumulation than DMEM/F12 (55 µM) (Figure 3). Critically, basal-subtracted analysis revealed net IBMX-induced melanin reached 0.0322 (high-glucose DMEM) versus 0.0165 (DMEM/F12) – a 95.2% enhancement attributable solely to tyrosine availability. This establishes media tyrosine standardization as the non-negotiable foundation for reproducible pigmentation studies.

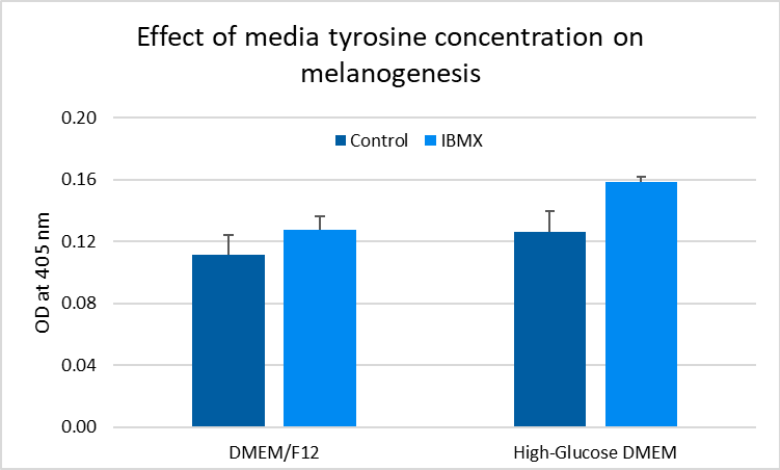

Figure 3. Tyrosine concentration dictates melanogenic output in IBMX-stimulated B16-F10 cells. IBMX-induced melanin showed 95.2% greater accumulation in high-tyrosine high-glucose DMEM (104 µM tyrosine*)* versus DMEM/F12 (55 µM tyrosine) under standardized induction (100 µM IBMX, 48h). Absolute optical densities: DMEM/F12 Control = 0.1112, IBMX = 0.1278; High-glucose DMEM Control = 0.1261, IBMX = 0.1583. Data represent mean and SD; n=*4* (two independent experiments, *two* replicates).

3.1.3. Kojic Acid Validation Benchmark

Melanin synthesis

Kojic acid (100-200 µM) demonstrated no intrinsic effect on basal melanogenesis in unstimulated B16-F10 cells (Figure 4a). Under IBMX induction (100 µM, 48h), which increased intracellular melanin by 142% versus control ($p<0.05$), kojic acid dose-dependently suppressed this stimulated melanogenesis:

- 100 µM: 58% inhibition of IBMX-induced melanogenesis ($p<0.01$)
- 200 µM: 87% inhibition ($p<0.01$)

This response profile validates kojic acid as a benchmark inhibitor, confirming the model's capacity to quantify dose-dependent depigmentation efficacy (Figure 4a). Critically, the 87% inhibition at 200 µM aligns with established potency ranges for tyrosinase inhibition (60–90% in published B16-F10 models).

Tyrosinase enzyme activity

Kojic acid (100-200 µM) exhibited distinct effects under basal versus stimulated conditions (Figure 4b):

- Basal state: Reduced intrinsic tyrosinase activity by 20% at both concentrations ($p<0.05$) without affecting melanin content.
- IBMX-stimulated state: IBMX alone increased tyrosinase activity by 46% versus control ($p<0.001$). Kojic acid suppressed this IBMX-induced enzyme activation by 16% (100 µM) and 23% (200 µM, $p<0.01$).

The disproportionate suppression of melanin synthesis (3.78 fold greater than enzyme inhibition) indicates kojic acid's secondary interference with melanosome maturation beyond direct tyrosinase inhibition, consistent with its known multi-target activity (Fig. 4b).

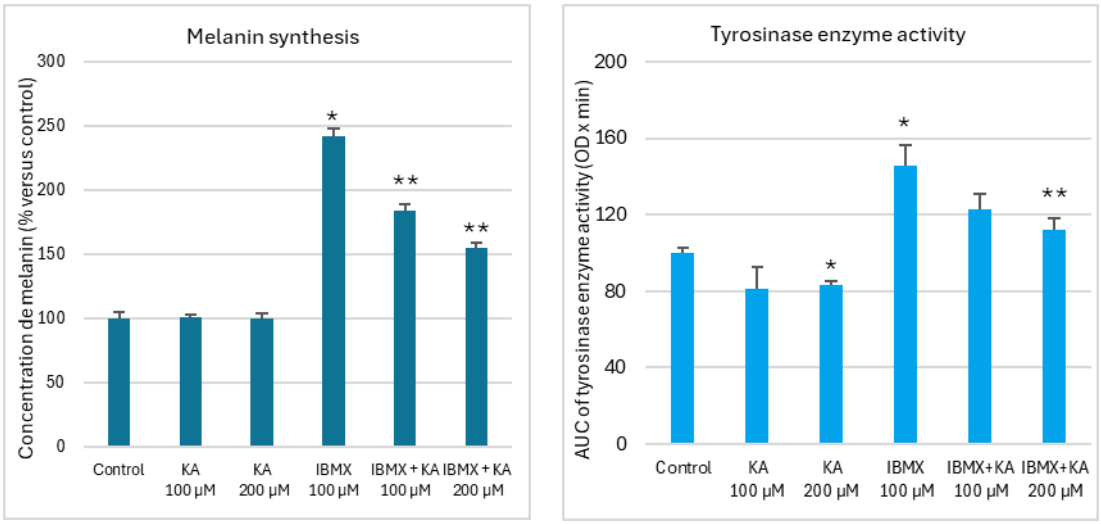

(**a**) (**b**)

Figure 4. Kojic acid inhibits IBMX-stimulated melanogenesis and tyrosinase activity in B16-F10 cells. (a) Melanin content under basal and IBMX-stimulated (100 µM, 48 h) conditions ± kojic acid (KA, 100-200 µM). IBMX increased melanin by 142% vs. control (*p<0.05 vs Control). KA dose-dependently suppressed IBMX-induced melanogenesis (58% inhibition at 100 µM, 87% at 200 µM; **p<0.01 vs. IBMX alone), without affecting basal melanogenesis. (b) Tyrosinase activity under basal and IBMX-stimulated conditions ± KA. IBMX increased activity by 46% vs. control (*p<0.05). KA reduced basal activity by 20% (*p<0.05) and suppressed IBMX-induced activity by 16% (100 µM) and 23% (200 µM; **p<0.01 vs. IBMX alone). Data represents mean and SD (n=20, melanin synthesis; n=8, tyrosinase activity).

3.1.4. Tyrosinase Knockdown Validation via siRNA

Targeted gene silencing confirms tyrosinase as the dominant regulatory node in IBMX-stimulated melanogenesis. Transfection of B16-F10 cells with *Tyr*-specific siRNA achieved significant suppression of tyrosinase expression, reducing mRNA levels by 53% versus scrambled siRNA controls (Figure 5a). This partial molecular knockdown translated into a disproportionately robust functional phenotype: melanin synthesis was suppressed by 75% under IBMX stimulation (Figure 5b).

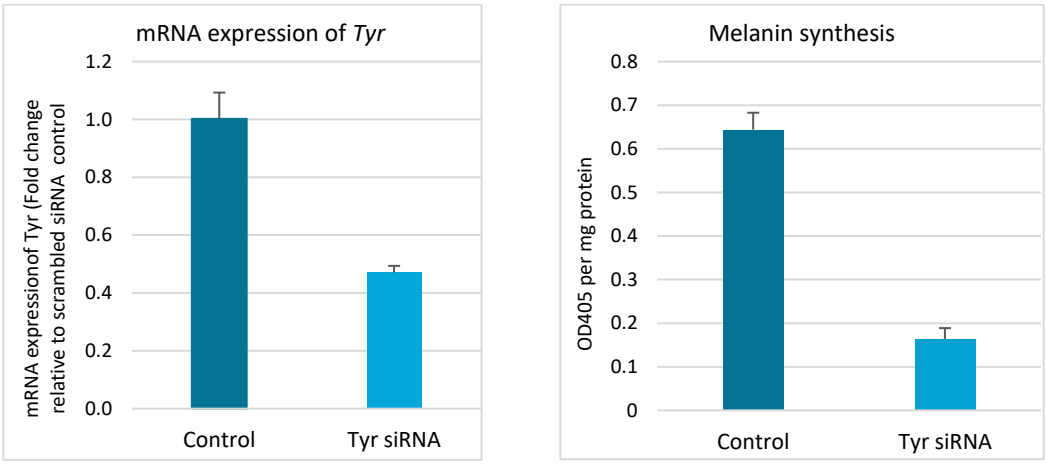

(**a**) (**b**)

Figure 5. siRNA-mediated tyrosinase (*Tyr*) knockdown suppresses IBMX-induced melanogenesis in B16-F10 cells. (a) *Tyr* mRNA expression 48h post-transfection (qPCR, normalized to *GAPDH*). (b) Melanin content (OD 405 nm, normalized to total protein) under IBMX stimulation. Data represent mean and SD. scrambled siRNA control; n=2 biological replicates.

3.1.5. Anti-Melanogenic Efficacy of *Willaertia* C2c Maky Lysate

Willaertia magna C2C Maky lysate (*Willaertia* lysate) suppresses IBMX-induced melanogenesis in a dilution-dependent manner, with maximal efficacy at 10^{-3}% rivaling the benchmark inhibitor kojic acid.

Tyrosinase Activity:

IBMX stimulation significantly increased intracellular tyrosinase activity by 49% versus unstimulated controls ($p < 0.001$). *Willaertia* lysate dose-dependently attenuated this hyperactivity (Figure 5a), achieving significant inhibition at all tested dilutions: 7% at 10^{-5} % ($p < 0.05$), 11% at 10^{-4} % ($p < 0.01$), and 9% at 10^{-3} % ($p < 0.05$). Notably, suppression at 10^{-4} % (11%) was statistically equivalent to kojic acid (15%, $p = 0.1$), indicating equivalent potency at this concentration.

Melanin Synthesis:

Consistent with its tyrosinase-inhibitory effects, *Willaertia* lysate treatment induced significant concentration-dependent reduction of IBMX-driven melanogenesis (Figure 6b): 12% decrease at 10^{-4} % ($p < 0.05$) and 22% decrease at 10^{-3} % ($p < 0.01$), with no significant effect at 10^{-5} % ($p > 0.05$). The 22% melanin inhibition at 10^{-3} % lysate closely matched the efficacy of kojic acid (24%), confirming potent dose-dependent anti-pigmentary activity.

The coordinated reduction in both tyrosinase activity and melanin synthesis demonstrates *Willaertia* lysate's functional efficacy in disrupting IBMX-driven melanogenesis.

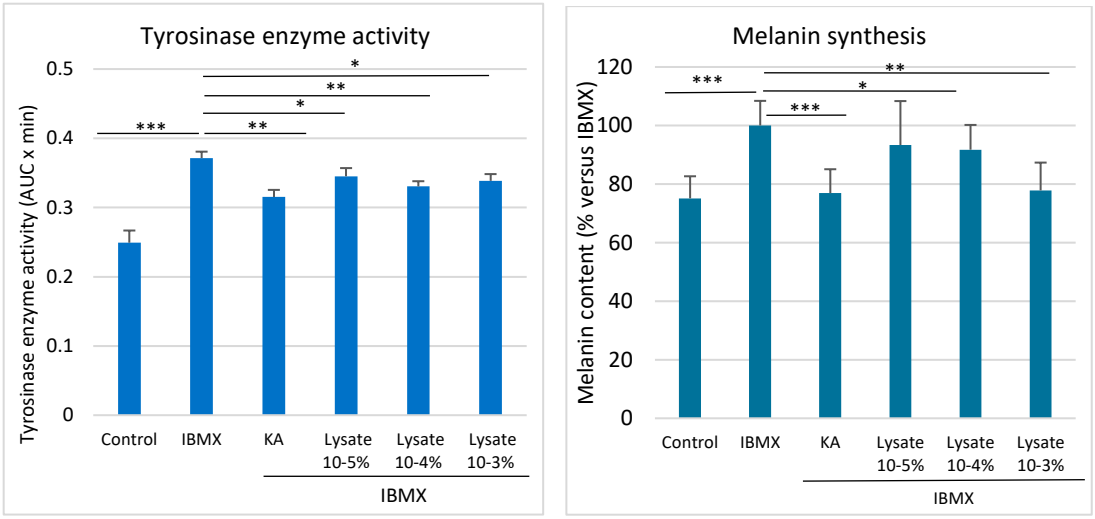

(**a**) (**b**)

Figure 6. *Willaertia* lysate suppresses IBMX-induced melanogenesis through dual inhibition of tyrosinase activity and melanin synthesis. (a) Tyrosinase Activity: IBMX stimulation (100 µM, 48 h) significantly increased tyrosinase activity vs. control. Both kojic acid (KA, 200 µM) and *Willaertia* lysate attenuated this induction, with lysate showing dose-dependent inhibition. (b) Melanin Synthesis: Kojic acid (KA) reduced IBMX-driven melanin accumulation by 24%. *Willaertia* lysate significantly decreased melanin at 10^{-4}% and 10^{-3}%, with 10^{-3}% matching KA efficacy. Data represent mean and SD, n=3 biological replicates; *p < 0.05, **p < 0.01, **p < 0.001.

4. Discussion

Our study first established a robust, physiologically relevant *in vitro* model of melanogenesis using IBMX-stimulated B16-F10 cells (Figures 1-2). IBMX, a phosphodiesterase inhibitor, elevates intracellular cAMP and potently induces melanin synthesis by upregulating microphthalmia-associated transcription factor (MITF) and its downstream targets, including tyrosinase (Tyr) – consistent with established mechanisms [9].

A critical methodological insight emerged from Figure 3: melanogenic output is profoundly sensitive to extracellular tyrosine concentration. This highlights the necessity of standardizing tyrosine levels in culture media during inhibitor screening – a variable often overlooked, potentially leading to misinterpretation of compound efficacy. Our optimized protocol ensures results reflect true inhibitory activity rather than substrate limitation artifacts.

The model's validity was rigorously confirmed using orthogonal approaches: (1) Kojic acid (Figure 4), a canonical Tyr inhibitor acting via copper chelation [10], exhibited a dose-dependent melanin reduction without cytotoxicity at effective concentrations, aligning with its established profile. (2) Genetic knockdown of Tyr via siRNA (Figure 5) significantly suppressed melanogenesis, directly confirming Tyr's indispensable role in our system. The concordance between pharmacological (kojic acid) and genetic (siRNA) inhibition solidifies the model's reliability for screening novel agents.

The central finding of this study is the potent, dose-dependent melanogenesis-inhibitory activity of *Willaertia* lysate (Figure 6). This represents the first report, to our knowledge, of melanogenic modulation by this protozoan species. The lysate achieved significant melanin reduction, demonstrating comparable or potentially superior potency to kojic acid within the non-toxic concentration range.

The mechanism of action remains to be fully elucidated. Based on the model validation (Figures 4-5), potent inhibition likely involves targeting the Tyr enzyme or its upstream regulators (e.g., MITF). However, the lysate's complex composition opens possibilities for multi-target effects distinct from kojic acid's direct Tyr chelation – potentially offering advantages in overcoming limitations like instability or reduced efficacy *in vivo* seen with some existing inhibitors [Rhododendrol].

The discovery of anti-melanogenic activity in *Willaertia* lysate expands the search for novel depigmenting agents beyond traditional botanical or synthetic sources. Protozoan represent an underexplored reservoir of bioactive molecules with potential applications in treating hyperpigmentation disorders (e.g., melasma, post-inflammatory hyperpigmentation) or in cosmetic skin lightening.

The potency of the crude lysate is particularly promising. Purification could yield a highly active single compound or synergistic fraction, potentially surpassing current options in efficacy or stability.

This work reinforces the importance of standardized, rigorously validated cellular models (Figures 1-3) for accurate evaluation of melanogenesis modulators. Our emphasis on tyrosine standardization provides a critical methodological framework for future studies.

Future Research Directions

Immediate priorities include determining the precise molecular target(s). Cell-free assays using mushroom or recombinant human tyrosinase will distinguish direct enzyme inhibition from effects on Tyr expression (MITF/Tyr mRNA/protein analysis) or cellular processing. Proteomic/metabolomic analysis of the lysate is essential to identify the active component(s). moreover, fractionation of the lysate guided by melanin inhibition and cytotoxicity assays is crucial to isolate the active principle(s), determine its structure, and assess stability. On the other hand, evaluation in normal human epidermal melanocytes (NHEMs) is imperative to confirm

activity and safety in a human-relevant, non-cancerous system, addressing limitations of the B16-F10 model. Longer-term exposure studies are needed.
Given the multi-target potential, investigating synergy between W. *magna* C2c Maky components and established inhibitors (e.g., kojic acid, arbutin) could lead to enhanced efficacy at lower, safer doses. Finally, this finding warrants broader screening of other protozoan species for melanogenesis-modulating activities.

5. Conclusion

In conclusion, we have established and validated a robust B16-F10 model for melanogenesis inhibition studies, highlighting the critical role of tyrosine standardization. This model is currently implemented in our cosmetic screening pipeline, enabling rapid prioritization of actives for clinical evaluation. Using this model, we identified *Willaertia* lysate as a potent novel inhibitor of melanin synthesis. While the active components and precise mechanism require further investigation, this discovery opens a promising avenue for developing new therapeutic agents for hyperpigmentation disorders from an unexplored biological source.

References

1- Global market data: Grand View Research (2023). Hyperpigmentation Treatment Market Size. Report ID: GVR-4-68040-308-4.
2- Ando H, Kondoh H, Ichihashi M, Hearing VJ. Approaches to identify inhibitors of melanin biosynthesis via the quality control of tyrosinase. J Invest Dermatol. 2007 Apr;127(4):751-61. doi: 10.1038/sj.jid.5700683.
3- Pillaiyar T., Manickam M., Namasivayam V. Skin whitening agents: Medicinal chemistry perspective of tyrosinase inhibitors. J. Enzym. Inhib. Med. Chem. 2017;32:403–425. 10.1080/14756366.2016.1256882.
4- Bustamante J; Breseston L; Malanga G; Mordoh, J. Role of Melanin as a Scavenger of Active Oxygen Species. Pigment Cell Research. 1993; 6(5):348-353
5- Lee Y, Song H-Y, Byun E-B. Anti-melanogenic effects of hydroxyethyl chrysin through the inhibition of tyrosinase activity: In vitro and in silico approaches. Heliyon, 2025; 11, e41718, doi.org/10.1016/j.heliyon.2025.e41718.
6- Kippenberger S, Loitsch S, Solano F, Bernd A, Kaufmann R. Quantification of Tyrosinase, TRP-1, and TRP-2 Transcripts in Human Melanocytes by Reverse Transcriptase-Competitive Multiplex PCR – Regulation by Steroid Hormones. Journal of Investigative Dermatology. 1998; 110, 364-367, doi.org/10.1038/jid.1998.1.
7- Buscà R, Ballotti R. Cyclic AMP a key messenger in the regulation of skin pigmentation. Pigment Cell Res. 2000 Apr;13(2):60-9. doi: 10.1034/j.1600-0749.2000.130203.x.
8- Kim K, Huh Y, Lim K-M. Anti-Pigmentary Natural Compounds and Their Mode of Action. International Journal of Molecular Sciences. 2021; 22(12):6206. https://doi.org/10.3390/ijms22126206.
9- Dos Santos M, Rorteau J, Laho K, Osman-Ponchet H, Barthe M, Quelard B, Carlino A, Saha A, Troussieux S. Willaertia Lysate: A Hydrobiome-Biosourced Ingredient with Multi-Site Antioxidative and Antiaging Properties. Cosmetics. 2024; 11(6):200. https://doi.org/10.3390/cosmetics11060200
10- Kim HD, Choi H, Abekura F, Park JY, Yang WS, Yang SH, Kim CH. Naturally-Occurring Tyrosinase Inhibitors Classified by Enzyme Kinetics and Copper Chelation. Int J Mol Sci. 2023 May 5;24(9):8226. doi: 10.3390/ijms24098226.